Journal of Thermal Analysis and Calorimetry, Vol. 89 (2007) 3, 681–686

THERMAL STABILITY OF AMPHIPHILIC DI-BLOCK COPOLYMER MONOLAYER

S. Y. Jung[1] *and H. Yoshida*[1,2]*

[1]Department of Applied Chemistry, Graduate School of Urban Environmental Science, Tokyo Metropolitan University Hachiouji, Tokyo 192-0397, Japan
[2]CREST (JST)

Monolayers of amphiphilic di-block copolymer, PEO_{40}-*b*-$PMA(Az)_{19}$ on water surface and solid surfaces, such as silicon wafer and quartz glass, were analyzed by surface pressure – molecular area (π–A) isotherm, UV-Vis spectroscopy, atomic force microscopy (AFM) and total X-ray reflectivity (TXR). The monolayer prepared at 22 mN m^{-1} consisted of H aggregated azobezene (Az) moieties, which orientated perpendicular to the solid surface. The monolayer structure, including H aggregated Az and orientation of Az, was stable after annealing at 98°C, at which temperature the hydrophilic PEO domain was the liquid phase and the hydrophobic PMA(Az) was in the smectic A phase.

Keywords: *amphiphilic di-block copolymer, azobenzene, H aggregation, monolayer, morphology, orientation, total X-ray reflectivity*

Introduction

Nano-scale structure controlled materials (nanomaterials) has paid a great deal of attention because of their potential applications in various areas such as electronics, optics, catalysis and nanocomposites [1, 2]. Block copolymer is one of these nanomaterials to form various interesting nano-scale ordered structure, such as body-centered cubic shear, hexagonal packed cylinder, bicontinuous gyroid and lamella, depending on volume fraction of component, interaction between components and degree of polymerization [3]. These nano-scale structures is a result of self-assembly of intramolecular phase separated block copolymer chains.

Langmuir–Blodgett (LB) technique is another method to produce nanomaterials by trapping monolayers kinetically in a predetermined arrangement, such as head-head alignment (Y membrane) and head-tail alignment (X and Z membranes). Not only LB technique but also the layer-by-layer deposition technique is used to form nanomaterial assembly. Bi-molecular layer structure of cell membrane is one of ideal nanomaterials having flexibility, structure stability and sufficient mechanical strength as a dynamic separator wall between outside and inside of cell, which transfer materials and information. The behavior of Langmuir (L) membrane of amphiphilic compounds, such as surfactants, on water surface is understandable through a surface pressure and surface area (π–A) isotherm. The molecular interaction at the interface between water and air works toward the specified direction, which differs from that of bulk state [4]. Not only surfactants but also amphiphilic polymers form L membrane on water surface. The L monolayer structures of weak and strong acid type electrolyte di-block copolymers [5, 6], polyelectrolytes [7] and amphiphilic di-block copolymers [8] on water surface are reported. Molecular cross section of hydrophobic component and thickness of monolayer are evaluated by π–A isotherm and total X-ray reflectivity (TXR), respectively.

L monolayer and LB membrane on solid surface are stabilized by the interaction with solid surface. We have reported the LB membrane structure of amphiphilic di-block copolymer consisted of hydrophilic polyethyleneoxide (PEO) and polymethacrylate having azobenzene (Az) moieties, PEOm-*b*-PMA(Az)n [9]. The surface structure of PEOm-*b*-PMA(Az)n LB membrane is consisted of the aligned hydrophobic PMA(Az)n domains, which is normal to the compression direction. As PEOm-*b*-PMA(Az)n forms the hexagonal packed PEO cylinder as an equilibrium structure [10–12], LB membrane of PEOm-*b*-PMA(Az)n is considered the quasi-equilibrium state [9]. Thermal stability of LB membrane of Az containing fatty acid was investigated by ultraviolet-visible (UV-Vis), infrared and fluorescence spectra [13]. The LB structure changes by the transformation of Az aggregates [13]. In this study, the thermal stability of PEOm-*b*-PMA(Az)n monolayer on silicon wafer and quartz glass was investigated by TXR and UV spectroscopy.

* Author for correspondence: yoshida-hirohisa@c.metro-u.ac.jp

1388–6150/$20.00

Akadémiai Kiadó, Budapest, Hungary
Springer, Dordrecht, The Netherlands

Experimental

Samples

PEO_{40}-*b*-$PMA(Az)_{19}$ di-block copolymer (Scheme 1) was synthesized from PEO macroinitiator and methacrylate derivative having azobenzene moieties in ester group by atom transfer radical polymerization [12] was used in this study. Degree of polymerization of PEO (m) and PMA(Az) (n) were 40 and 19, respectively. The degree of dispersion determined by GPC was 1.14.

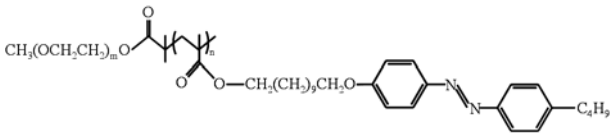

Scheme 1

The PEO_{40}-*b*-$PMA(Az)_{19}$ monolayers prepared on quartz glass and silicon wafer were annealed as the following thermal history. Monolayer was heated from room temperature to 98°C at 1 K min^{-1}, and hold for 1 h at 98°C, then cooled to room temperature at 1 K min^{-1}.

Measurements

Surface pressure and molecular area (π–A) isotherm was measured by compressing PEO_{40}-*b*-$PMA(Az)_{19}$ monolayer prepared by evaporation from the chloroform solution of PEO_{40}-*b*-$PMA(Az)_{19}$ (1 mmol L^{-1} Az $unit^{-1}$) on distilled water surface at a speed of 10 mm min^{-1} using Wilhelm plate (LB240-S-MWC, Filgen Ltd., Japan) at 23°C. Monolayer was deposited on quartz glass and silicon wafer at various pressure (1, 4, 7, 15, 22, 24, 28 mN m^{-1}) and the obtained monolayer was kept in a desiccator at room temperature.

The phase transitions were measured by a differential scanning calorimeter (DSC6200, Seiko Instruments Co. Ltd.) with a cooling apparatus in dry nitrogen atmosphere. The sample mass and scanning rate was 3 mg and 10 K min^{-1}, respectively.

Total X-ray reflectivity (TXR) of LB membrane on silicon wafer was measured in the θ/2θ reflection mode by a Mac-Science MXP21 operating at 40 kV and 300 mA. The range of 2θ scanning was from 0.5 to 8° at 0.2° min^{-1}, respectively. Ultraviolet-visible (UV-Vis) absorption measurement of PEO_{40}-*b*-$PMA(Az)_{19}$ monolayer on quartz glass was performed by UV-Vis spectrometer (V-6500, JASCO, Japan) at room temperature.

In order to observe the surface structure of monolayer on silicon wafer, atomic force microscope measurement was carried out by WET-SPM-9500 J3, Shimadzu equipped with a Veeco-TAP150 tip in contact mode.

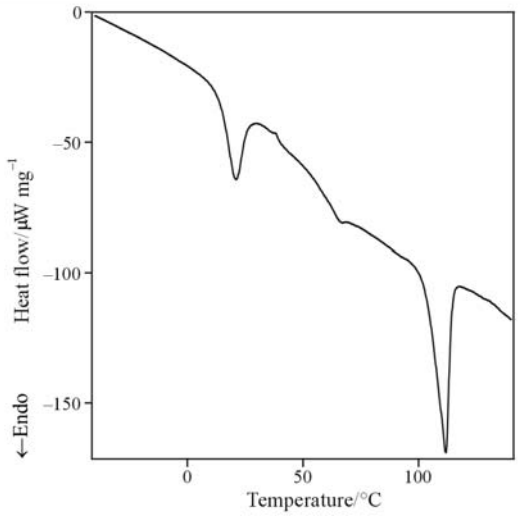

Fig. 1 DSC heating curve of PEO_{40}-*b*-$PMA(Az)_{19}$ at 10 K min^{-1}

Results and discussion

Figure 1 shows DSC heating curve of PEO_{40}-*b*-$PMA(Az)_{19}$ bulk sample. Four endothermic peaks were observed at 14, 53, 83 and 103°C, were assigned to the melting of PEO domain, the transitions from smectic X to smectic C (SmC), from SmC to smectic A (SmA) and from SmA to isotropic liquid-state [10, 11].

Figure 2 shows π–A isotherm of PEO_{40}-*b*-$PMA(Az)_{19}$ at 23°C. The molecular area was shown in the area per methacrylate repeating unit. Two types of molecular cross section area were evaluated, one was the area at 22 mN m^{-1} and the other was the area extrapolating π–A curve in the 2-dimensional

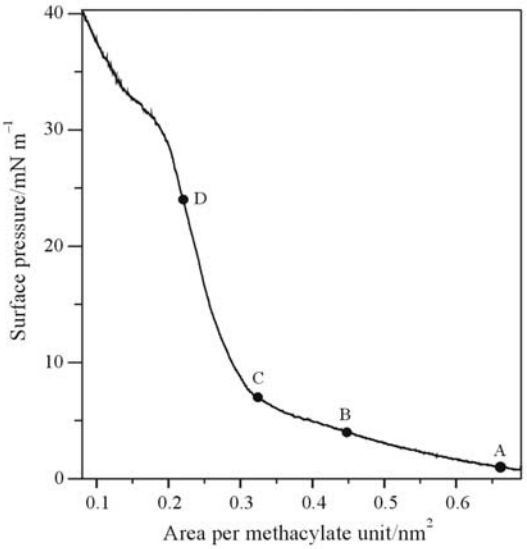

Fig. 2 Surface pressure – molecular area (π–A) isotherm of PEO_{40}-*b*-$PMA(Az)_{19}$ monolayer at 23°C. Points from A to D indicated the monolayer prepared pressures on silicon wafer for AFM observation

solid-state to zero surface pressure. The former was 0.22 (A_{22}) and the later was 0.32 (A_0) nm^2, respectively. The diameter of hydrophobic domain of single PEO_{40}-*b*-$PMA(Az)_{19}$ molecule (2R) and the distance between close-neighboring PMA(Az) units (D) calculated from A_0 and A_{22} were 2.75 (2R from A_0), 2.3 (2R from A_{22}), 0.63 (D from A_0) and 0.52 (D from A_{22}) nm, respectively. The 2R value calculated from A_{22} (2.3 nm) showed a good agreement with the 2R of $PMA(Az)_{19}$ domain on the LB surface of PEO_{40}-*b*-$PMA(Az)_{19}$, however, the value of D value obtained from A_{22} (0.52 nm) was slightly larger than the value between Az moieties (0.4 nm) in the bulk state and LB membrane [9].

Figure 3 shows AFM phase images of PEO_{40}-*b*-$PMA(Az)_{19}$ monolayer prepared at various surface pressure (π), 1 (a), 4 (b), 7 (c) and 24 (d) mN m^{-1}. The height profile of AFM topological image was shown above each AFM phase images. Figure 3a, corresponding to 2-dimensional gas phase, showed ring like structure which was consisted of small particles (the size of particles were smaller than the space resolution of AFM under the experimental condition). The average distance between ring like structures was about 50 nm. The height profile of gas phase indicated the height gap of ring structure was about 3 nm, which corresponded to the length of ester group in PMA(Az). Figure 3b, corresponding to 2-dimensional liquid expanded phase, showed closed-packed short rods with 20–30 nm width and various lengths. The height profile of the liquid phase showed these length and width of rods, indicating random orientation of rods with about 3 nm height gap. From AFM images shown in Figs 3a and b, the coagulations consisted of few PEO_{40}-*b*-$PMA(Az)_{19}$ molecules were approached each other with the increase of π and transformed to 2-dimensional liquid expanded phase. In the transition region from gas to liquid, the ring like structures were collapsed and changed to the rod structures. Then the rod like coagulations packed closely in the liquid-state. Figure 3c, corresponding to the transition region from liquid expanded to condensed phase, indicated that the rod like structures were collapsed and the height gap decreased to 2–0.5 nm. Figure 3d, corresponding to the 2-dimensional liquid condensed phase, the surface became flat with 0.5 nm height gap. No ordered surface structure was observed both in the liquid and solid-state.

Figure 4 shows UV-Vis absorption spectra of PEO_{40}-*b*-$PMA(Az)_{19}$ monolayers on quartz substrate at various surface pressure. UV-Vis spectroscopic data clearly reveal differences in the aggregation and the out of plane orientation of Az units in the monolayer of different lateral packing density. The UV-Vis spectra of toluene solution of PEO_{40}-*b*-$PMA(Az)_{19}$ showed two characteristic absorption peaks at 245 and 350 nm, these bands were assigned to the orientation independent ϕ–ϕ* of aromatic ring and the orientation dependent π–π* transitions of aromatic core of Az unit, respectively [14]. The transition moment of ϕ–ϕ* (245 nm) and π–π* (350 nm) transitions are parallel to the short axis and the long axis or Az unit, respectively. The absorption spectra of monolayer (A, B and C) showed the blue shift of π–π* band from 350 to 320 nm compared to that of toluene solution. This blue shift suggested H aggregation of Az units, in which Az units aligned side-by-side in monolayer, H aggregation of Az were reported for LB membranes of compounds including Az units [15, 16]. As UV-Vis spectrum of monolayer showed the shoulder at 350 nm, both H aggregated Az and random Az were existed in PEO_{40}-*b*-$PMA(Az)_{19}$ monolayer, the relative absorbance of peaks at 320 and 350 indicated the relative amount of H aggregated Az and random Az. The relative absorbance of peaks at 320 and 245 nm (A_{245}/A_{320}) indicated the out of plane

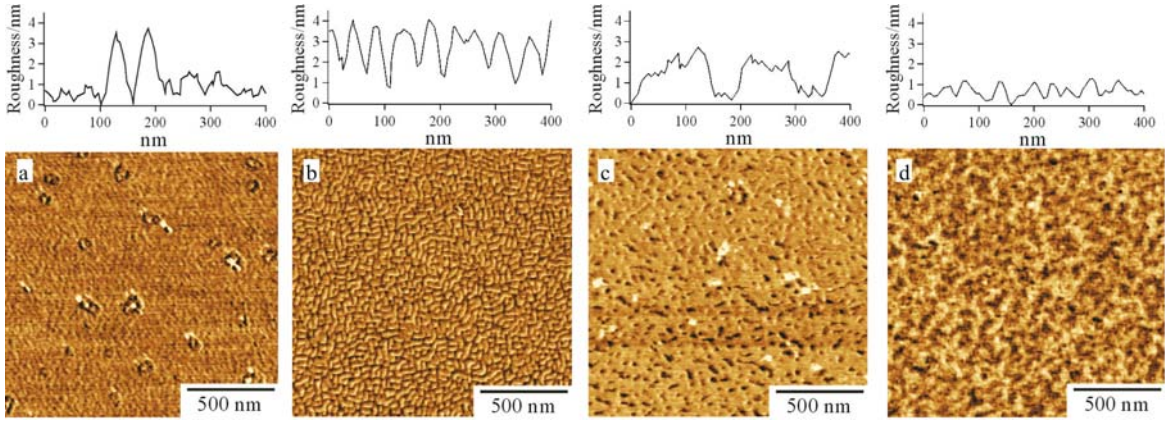

Fig. 3 AFM phase images of monolayer prepared at various phases, a – 2-dimensional gas phase (π=1 mN m^{-1}), b – 2-dimensional liquid expanded phase (π=4 mN m^{-1}), c – transition region from 2-dimensional liquid expanded phase to 2-dimensional condensed phase (π=7 mN m^{-1}) and d – 2-dimensional condensed phase (π=24 mN m^{-1}). Height profiles of topo images were shown above each AFM phase images

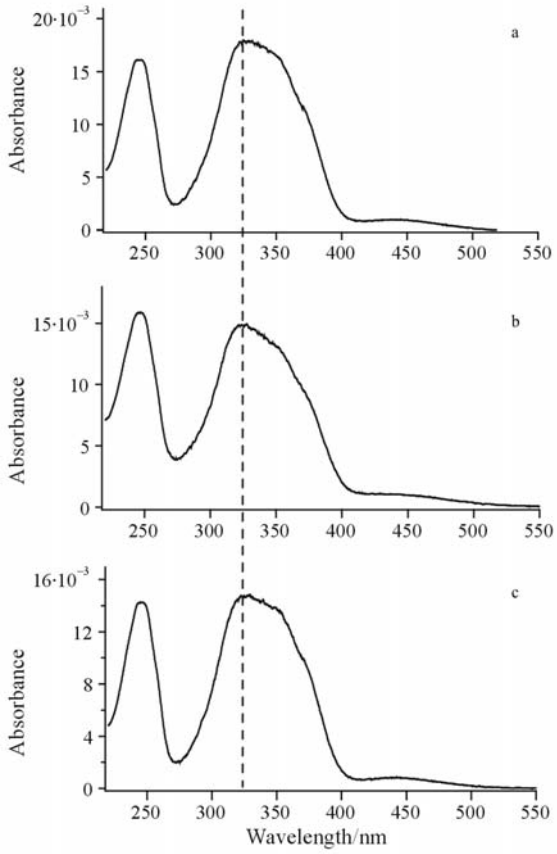

Fig. 4 UV-Vis spectra of PEO_{40}-*b*-$PMA(Az)_{19}$ monolayer prepared at various surface pressures corresponding to 2-dimensional condensed phase, a – π=15, b – π=22 and c – π=24 mN m^{-1}

orientation of Az units. The A_{245}/A_{320} value of monolayers prepared at 15 (a), 22 (b) and 24 (c) mN m^{-1} were 0.885, 1.066 and 0.962, respectively. The monolayer (b) prepared at 22 mN m^{-1} showed the highest orientation state of (Az) moieties and the lowest content of random (Az) moieties.

Figure 5 shows the total X-ray reflective (TXR) profiles of PEO_{40}-*b*-$PMA(Az)_{19}$ monolayer prepared at various surface pressures on silicon wafer. TXR profiles of monolayers showed fringes due to the interference of reflective X-ray beams at each surfaces. TXR intensity $I(2\theta)$ from multi-layer structure is written by the following equation [17].

$$I(2\theta)=\left(\frac{\delta_1}{2\theta^2}\right)^2+\sum\left(\frac{\delta_i-\delta_{i-1}}{2\theta^2}\right)^2+$$
$$\sum\left(\frac{\delta_{i-1}}{2\theta^2}\right)\left(\frac{\delta_i-\delta_{i-1}}{2\theta^2}\right)\cos(4\pi_{i-1}\sqrt{\sin^2\theta-2\delta_{i-1}})+$$
$$\sum\left(\frac{\delta_{i-1}}{2\theta^2}\right)\left(\frac{\delta_i-\delta_{i-1}}{2\theta^2}\right)\cdot$$
$$\cos\left(4\pi(t_{i-1}+t_i)\sqrt{\sin^2\theta-2\frac{t_{i-1}\delta_{i-1}+t_i\delta_i}{t_{i-1}+t_i}}\right)$$

where δ and t indicate the density and thickness of i^{th} layer, respectively. The PEO_{40}-*b*-$PMA(Az)_{19}$ monolayer was assumed to consist of four layers, chain end alkyl group (a), (Az) (b), PMA (c) and PEO (d) on silicon surface. The profile fitting result was shown in Fig. 6, and the density and thickness of each layers in monolayer was shown in Table 1. The profile fitting results suggested that the PEO_{40}-*b*-$PMA(Az)_{19}$ monolayer consisted of four independent layers and Az moieties (b) aligned perpendicular to silicon surface, which agreed with UV-Vis spectra. The obtained profile showed a good agreement with the experimental TXR profile, however, the obtained density of (Az) layer (b, 1.25 g cm^{-1}) was higher than the crystal density of (Az) (1.2 g cm^{-1}). The discrepancy was a result of complex model of monolayer comparing to the simple TXR profile. Therefore, we evaluated only the total thickness of monolayer membrane from TXR profile. The total thickness of monolayers prepared at 15 (a), 22 (b) and 28 (c) mN m^{-1} were 3.71, 4.16 and 5.81 nm, respec-

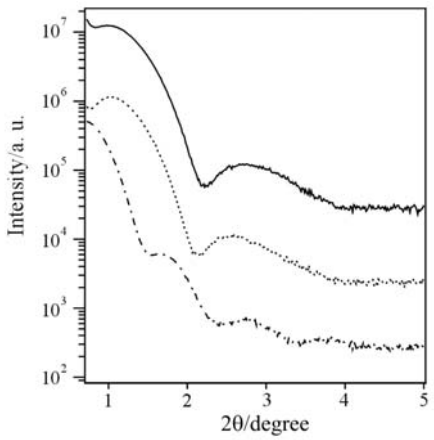

Fig. 5 Total X-ray reflective profiles of PEO_{40}-*b*-$PMA(Az)_{19}$ monolayer prepared at various surface pressures corresponding to 2-dimensional condensed phase, a – π=15, b – π=22 and c – π=28 mN m^{-1}

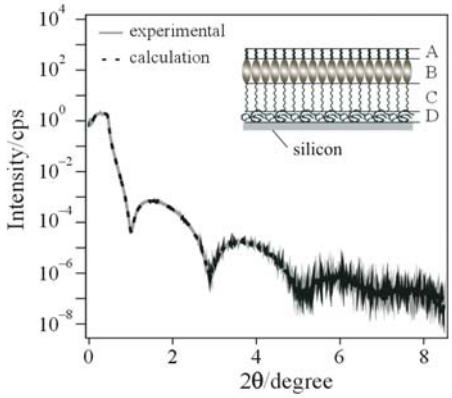

Fig. 6 Model fitting of total X-ray reflectivity result for PEO_{40}-*b*-$PMA(Az)_{19}$ monolayer prepared at π=24 mN m^{-1}

Table 1 Obtained thickness and density of each layers by model fitting of TXR profile

Layer	Thickness/nm	Density/g cm^{-3}
A	0.335	0.86357
B	1.140	1.25467
C	1.571	1.04845
D	1.626	0.95077

tively. These thickness were slightly larger than the ordered layer of LB membrane of PEO_{40}-*b*-$PMA(Az)_{19}$ (3.2 nm) and SmC layer thickness (3.3 nm) [18], which was consisted of bilayer of hydrophobic PMA(Az) [9] and Az molecules formed the interdigitated SmC structure [18].

Monolayer was annealed at 98°C, corresponding to the SmC phase of hydrophobic domain and the liquid phase of hydrophilic PEO domain, for 1 h to evaluate the thermal stability of monolayer structure. Figure 7 showed UV-Vis spectrum changes of monolayer before and after the annealing at 98°C. For the monolayer (a) prepared at 15 mN m^{-1}, the absorbance at 320 nm increased and the relative absorbance at 350 *vs.* 320 nm increased after the annealing, therefore some H aggregated Az moieties changed to random Az and the orientation degree of Az decreased by annealing. For the monolayer (b) prepared at 22 mN m^{-1}, the absorbance at 320 nm increased slightly and the relative absorbance at 350 *vs.* 320 nm decreased scarcely after the annealing. For the monolayer (c) prepared at 28 mN m^{-1} which corresponded to the pressure closed to the transition region from 2-dimensional solid monolayer to solid bi-molecular layer, the relative absorbance A_{245}/A_{320} decreased slightly after the annealing. These results indicated that the aggregation of Az moieties in monolayers b and c increased with the annealing and the orientation of Az scarcely decreased by the annealing.

Figure 8 showed TXR profile changes of monolayer by annealing at 98°C. All TXR profiles of annealed monolayer showed the similar profiles of unannealed monolayer shown in Fig. 5, therefore the smooth surface of monolayer remained after annealing. The total thickness changes by annealing were 3.71 to 5.19 nm (a), 4.16 to 6.59 nm (b) and 5.81 to 11.31 nm (c). The increment of monolayer thickness by annealing was 2.02 (a), 2.43 (b) and 5.5 nm. From

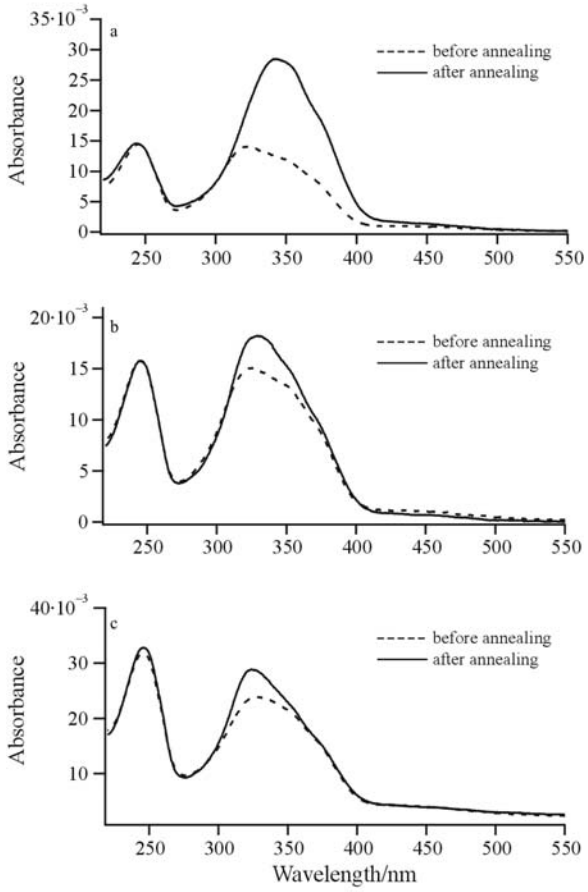

Fig. 7 UV-Vis spectra changes of PEO_{40}-*b*-$PMA(Az)_{19}$ monolayer by annealing at 98°C. Monolayers were prepared at various surface pressures, a – π=15, b – π=22 and c – π=28 mN m^{-1}

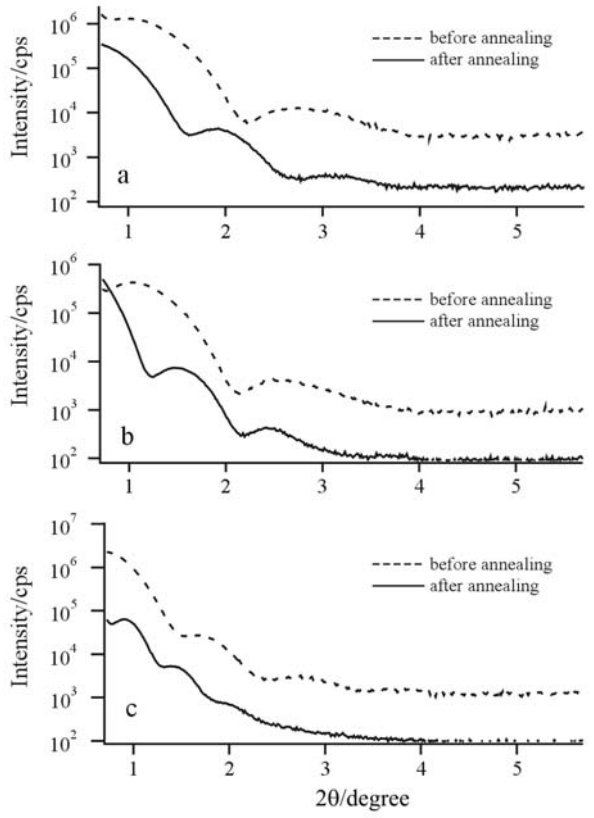

Fig. 8 Total X-ray reflective profiles changes of PEO_{40}-*b*-$PMA(Az)_{19}$ monolayer by annealing at 98°C. Monolayers were prepared at various surface pressures corresponding to 2-dimensional condensed phase, a – π=15, b – π=22 and c – π=28 mN m^{-1}

the model fitting results of TXR profile shown in Table 1, the thickness of hydrophilic PEO layer was about 1.6 nm, which was almost a half of the estimated thickness (2Rg=3.5 nm) from the radius of gyration of PEO_{40} unit (Rg=1.76 nm). This fact indicated that hydrophilic PEO part of PEO_{40}-*b*-$PMA(Az)_{19}$ shrunk in water due to lower solubility of PEO_{40} and formed thin PEO layer in monolayer. The shrunk PEO layer was expected to expand to 3.5 nm thickness by annealing, this was one of possibility to explain the increment of thickness for monolayer a and b. However, the thickness increment was almost the double for monolayer c, monolayer c changed bi-molecular layer by annealing.

Conclusions

Monolayer of PEO_{40}-*b*-$PMA(Az)_{19}$ was prepared on silicon wafer and quartz glass at various surface pressures. The H aggregation of Az formed at the transition region from the 2-dimensional liquid expanded phase to the 2-dimensional liquid condensed phase of L monolayer on water surface. The relative amount of H aggregation and the orientation of Az perpendicular to the solid surface were higher in the monolayer prepared at 22 mN m^{-1}. The monolayer structure was stable against the annealing at 98°C, corresponding to SmA phase of hydrophobic domain.

Acknowledgements

The authors are grateful to the Japan Science and Technology Agency for support of this research through Grant CREST 'Nano Factory'.

References

1 Z. L. Wang, Characterization of Nanophase Materials, Wiley-VCN, Weinheim 2000, p. 3.
2 N. A. Ktow, Multilayer Thin Films, Wiley-VCN, Weinheim 2003, p. 207.
3 I. W. Hamley, 'Developments in Block Copolymer Science and Technology' Ed. I. W. Hamley, John Wiley and Sons, Chichester 2004, p. 6.
4 K. Kurihara, K. Ohto, Y. Honda and T. Kunitake, J. Am. Chem. Soc., 113 (1991) 5077.
5 E. Mouri, K. Matsumoto, H. Matsuoka and H. Yamaoka, Langmuir, 18 (2002) 3865.
6 E. Mouri, K. Matsumoto and H. Matsuoka, J. Polym. Sci. B, 41 (2003) 1921.
7 H. Baltes, M. Schwendler, C. A. Helm, R. Heger and W. A. Goedel, Macromoleules, 30 (1997) 6633.
8 T. Kobayashi and T. Seki, Langmuir, 19 (2003) 9297.
9 S. Y. Jung and H. Yoshida, Colloids Surf. A, 284–285 (2006) 305.
10 K. Watanabe, Y. Tian, H. Yoshida, S. Asaoka and T. Iyoda, Trans. Mater. Res. Soc. Jpn., 28 (2003) 553.
11 H. Yoshida, K. Watanabe, R. Watanabe and T. Iyoda, Trans. Mater. Res. Soc. Jpn., 28 (2003) 861.
12 H. Yoshida, Netsu-Sokutei, 31 (2004) 553.
13 K. Taniike, T. Matsumoto, T. Sato, Y. Ozaki, K. Nakashima and K. Iriyama, J. Phys. Chem., 100 (1996) 15508.
14 B. Sapich, A. B. E. Vix, J. P. Rabe, J. Stumpe, G. Wilbert and R. Zentel, Thin Solid Films, 514 (2006) 165.
15 H. Tachibana, N. Yoshino and M. Matsumoto, Chem. Lett., (2000) 240.
16 T. Seki and K. Ichimura, Thin Solid Films, 179 (1989) 77.
17 T. C. Huang and W. Parrish, Adv. X-Ray Anal., 35 (1992) 137.
18 R. Watanabe, T. Iyoda, T. Yamada and H. Yoshida, J. Therm. Anal. Cal., 85 (2006) 713.

DOI: 10.1007/s10973-006-7955-x